

# Multi-Level Optimal Power Flow Solver in Large Distribution Networks

Xinyang Zhou, Yue Chen, Zhiyuan Liu, Changhong Zhao, and Lijun Chen

**Abstract**—We consider large multi-phase distribution networks of tree topology that can be divided into collaborating areas and subareas featuring subtree topology, and design a multi-level implementation of the primal-dual gradient algorithm for solving the optimal power flow problems while preserving nodal information within areas. Numerical results on a 4,521-node system verifies that such design significantly improves convergence speed without compromising optimality.

**Index Terms**—Distributed algorithms, voltage control, large-scale systems, gradient methods

## I. INTRODUCTION

With the emergence of smart electricity device, the size of related optimal power flow (OPF) problems grow considerably. Meanwhile, the increasing penetration of intermittent renewable energy generation in distribution networks leads to rapidly evolving system states and calls for fast OPF solving. These motivate researchers to look for scalable and efficient distributed OPF solvers [1]. However, existing distributed OPF solvers may lack scalability when the size of the problem increases with larger network and more controllable devices. For example, when the network is huge, the gradient-based centrally coordinated distributed OPF solver for the optimal voltage regulation problem suffers from the computational bottleneck of the centrally calculated part that couples the entire network [3], though some computation tasks based on local information are already distributed.

A promising line of works for this problem propose to divide a big network into smaller ones and thus to solve smaller parts of the OPF problems in collaboration instead of the original large ones [2]. However, existing works usually lose certain level of optimality when doing so—the original OPF problem is not equivalently solved—and lack numerical verification on large systems.

In this work we focus on distribution network featuring tree topology, which is known to have fractal properties: any

X. Zhou and Y. Chen are with Power System Engineering Department, National Renewable Energy Laboratory, Golden CO 80401, USA (Emails: {xinyang.zhou, yue.chen}@nrel.gov).

Z. Liu and L. Chen are with the College of Engineering and Applied Science, University of Colorado, Boulder, CO 80309, USA (Emails: {zhiyuan.liu, lijun.chen}@colorado.edu).

C. Zhao is with the Department of Information Engineering, the Chinese University of Hong Kong, HK (Emails: chzhao@ie.cuhk.edu.hk).

This work was authored in part by the National Renewable Energy Laboratory, operated by Alliance for Sustainable Energy, LLC, for the U.S. Department of Energy (DOE) under Contract No. DE-EE-0007998. Funding provided by U.S. Department of Energy Office of Energy Efficiency and Renewable Energy Solar Energy Technologies Office. The views expressed in the article do not necessarily represent the views of the DOE or the U.S. Government. The U.S. Government retains and the publisher, by accepting the article for publication, acknowledges that the U.S. Government retains a nonexclusive, paid-up, irrevocable, worldwide license to publish or reproduce the published form of this work, or allow others to do so, for U.S. Government purposes.

node within a tree together with all its children nodes makes a subtree that also features tree topology and thus inherits the same properties from the original tree; such properties are then passed on to subtrees within subtrees and so on. This observation motivates us to develop a framework to exploit such fractal pattern to improve the efficiency of solving OPF in large distribution networks.

Following our previous work [3], this work continues to explore the fractal properties of the distribution networks and reveal the corresponding patterns on the sensitivity matrices between voltage magnitudes and nodal power injections in a multi-phases system and proposes a multi-level solution method to solve optimal voltage regulation problems. The proposed algorithm significantly improves the efficiency of solving large convex OPF problems without losing optimality, as illustrated with numerical results based on a 4,521-node distribution system. Such highly efficient design is crucial for tracking the optimal operating setpoints in real time and fast recovery from blackout for large distribution systems with a large number of control nodes.

## II. SYSTEM MODEL AND OPF

### A. Network Modeling

Following [3], we consider a radial multi-phase distribution system denoted by  $\mathcal{G} = \{\mathcal{N} \cup \{0\}, \mathcal{E}\}$  with the set  $\mathcal{N}$  collecting all  $n$  buses excluding the substation bus 0 modeled as a slack bus, and the set  $\mathcal{E}$  collecting their connecting lines. We denote by  $\mathcal{E}_i$  the set of lines describing the unique path from the substation to bus  $i$ . Define  $i := \sqrt{-1}$ . Let  $a, b, c$  denote the three phases, and  $\Phi_i$  denote the set of phase(s) of node  $i \in \mathcal{N}$ . Obviously,  $\Phi_i \subseteq \Phi_0, \forall i \in \mathcal{N}$ . Define a subset  $\mathcal{N}^\phi \subseteq \mathcal{N}$  collecting buses that have phase  $\phi$ . Denote by  $p_i^\phi, q_i^\phi, V_i^\phi$  and  $v_i^\phi$  the real power injection, the reactive power injection, the complex voltage phasor, and the squared voltage magnitude, respectively, of phase  $\phi \in \Phi_i$  at bus  $i \in \mathcal{N}$ . We make the following assumptions for a linearized power flow model.

**Assumption 1** *The line losses are small and ignored, and the magnitudes of three-phase voltages are approximately equal and the phase differences among three-phase voltages are close to  $2\pi/3$ , i.e.,  $\frac{V_i^a}{V_i^b} \approx \frac{V_i^b}{V_i^c} \approx \frac{V_i^c}{V_i^a} \approx e^{i2\pi/3}$ .*

Denote by  $z_{\zeta\xi}$  the impedance of line  $(\zeta, \xi) \in \mathcal{E}$ , which is a complex number for a single-phase line, a  $2 \times 2$  complex matrix for a two-phase line, or a  $3 \times 3$  complex matrix for a three-phase line. Denote by  $Z_{ij}^{\varphi\phi} = \sum_{(\zeta, \xi) \in \mathcal{E}_i \cap \mathcal{E}_j} z_{\zeta\xi}^{\varphi\phi} \in \mathbb{C}$  the summarized impedance (if  $\varphi = \phi$ ) or the mutual impedance (if  $\varphi \neq \phi$ ) of the common path of buses  $i$  and  $j$  leading back to bus 0, and  $\overline{Z}_{ij}^{\varphi\phi}$  its conjugate. Define

$$\mathbf{v} := [[v_1^\phi]_{\phi \in \Phi_1}^\top, \dots, [v_n^\phi]_{\phi \in \Phi_n}^\top]^\top \in \mathbb{R}^N$$

$$\begin{aligned}\mathbf{p} &:= [[p_1^\phi]_{\phi \in \Phi_1}^\top, \dots, [p_n^\phi]_{\phi \in \Phi_N}^\top]^\top \in \mathbb{R}^N \\ \mathbf{q} &:= [[q_1^\phi]_{\phi \in \Phi_1}^\top, \dots, [q_n^\phi]_{\phi \in \Phi_N}^\top]^\top \in \mathbb{R}^N\end{aligned}$$

the vectors of the squared voltage magnitudes, the real power injection, and reactive power injection, with  $N = \sum_{i \in \mathcal{N}} |\Phi_i|$ . Here,  $|\Phi_i|$  is the cardinality of set  $\Phi_i$ . We use the following *linearized* power flow equation [4], [5]:

$$\mathbf{v} = \mathbf{R}\mathbf{p} + \mathbf{X}\mathbf{q} + \tilde{\mathbf{v}}, \quad (1)$$

with a constant vector  $\tilde{\mathbf{v}}$  and sensitivity matrices  $\mathbf{R}, \mathbf{X} \in \mathbb{R}^{N \times N}$  respectively comprising of elements of  $\partial_{p_j^\phi} v_i^\phi = 2\Re\{\bar{Z}_{ij}^{\varphi-\phi} \cdot \omega^{\varphi-\phi}\}$  and  $\partial_{q_j^\phi} v_i^\phi = -2\Im\{\bar{Z}_{ij}^{\varphi-\phi} \cdot \omega^{\varphi-\phi}\}$ . Here,  $\omega = e^{-i2\pi/3}$ ,  $a, b, c = 0, 1, 2$  when calculating  $\varphi - \phi$ , and  $\Re\{\cdot\}/\Im\{\cdot\}$  is the real/imaginary part of a complex number.

### B. Problem Formulation and Gradient Algorithm

We formulate a voltage regulation OPF problem for the multi-phase distribution system as follows:

$$\min_{\mathbf{p}, \mathbf{q}} \sum_{i \in \mathcal{N}} \sum_{\phi \in \Phi_i} C_i^\phi(p_i^\phi, q_i^\phi), \quad (2a)$$

$$\text{s.t. } \underline{\mathbf{v}} \leq \mathbf{v}(\mathbf{p}, \mathbf{q}) \leq \bar{\mathbf{v}}, \quad (2b)$$

$$(p_i^\phi, q_i^\phi) \in \mathcal{Y}_i^\phi, \phi \in \Phi_i, \forall i \in \mathcal{N}, \quad (2c)$$

where  $C_i^\phi$  is a jointly strongly convex function in both  $p_i^\phi$  and  $q_i^\phi$  for phase  $\phi \in \Phi$  of node  $i$ ,  $\mathcal{Y}_i^\phi$  is its convex and compact feasible set,  $\mathbf{v}(\mathbf{p}, \mathbf{q})$  represents Eq. (1), and  $\underline{\mathbf{v}} = \{\underline{v}_i^\phi\}_{i \in \mathcal{N}}^{\phi \in \Phi_i}$  and  $\bar{\mathbf{v}} = \{\bar{v}_i^\phi\}_{i \in \mathcal{N}}^{\phi \in \Phi_i}$  are the voltage bounds. Associate dual variables  $\underline{\boldsymbol{\mu}} = \{\underline{\mu}_i^\phi\}_{i \in \mathcal{N}}^{\phi \in \Phi_i}$  and  $\bar{\boldsymbol{\mu}} = \{\bar{\mu}_i^\phi\}_{i \in \mathcal{N}}^{\phi \in \Phi_i}$  with constraints (2b) and we write the regularized Lagrangian of (2) as:

$$\begin{aligned}\mathcal{L}(\mathbf{p}, \mathbf{q}; \bar{\boldsymbol{\mu}}, \underline{\boldsymbol{\mu}}) &= \sum_{i \in \mathcal{N}} \sum_{\phi \in \Phi_i} C_i^\phi(p_i^\phi, q_i^\phi) + \underline{\boldsymbol{\mu}}^\top (\underline{\mathbf{v}} - \mathbf{v}(\mathbf{p}, \mathbf{q})) \\ &\quad + \bar{\boldsymbol{\mu}}^\top (\mathbf{v}(\mathbf{p}, \mathbf{q}) - \bar{\mathbf{v}}) - \frac{\eta}{2} \|\boldsymbol{\mu}\|_2^2,\end{aligned} \quad (3)$$

with regularization term  $-\frac{\eta}{2} \|\boldsymbol{\mu}\|_2^2$  added to improve convergence properties.

We implement the primal-dual gradient algorithm for solving the unique saddle point of (3) with a stepsize  $\epsilon$  as:

$$p_i^\phi(t+1) = \left[ p_i^\phi(t) - \epsilon \left( \partial_{p_i^\phi} C_i^\phi(p_i^\phi(t), q_i^\phi(t)) + \sum_{j \in \mathcal{N}} \sum_{\varphi \in \Phi_j} \partial_{p_i^\phi} v_j^\varphi(\bar{\mu}_j^\varphi(t) - \underline{\mu}_j^\varphi(t)) \right) \right]_{\mathcal{Y}_i^\phi}, \quad (4a)$$

$$q_i^\phi(t+1) = \left[ q_i^\phi(t) - \epsilon \left( \partial_{q_i^\phi} C_i^\phi(p_i^\phi(t), q_i^\phi(t)) + \sum_{j \in \mathcal{N}} \sum_{\varphi \in \Phi_j} \partial_{q_i^\phi} v_j^\varphi(\bar{\mu}_j^\varphi(t) - \underline{\mu}_j^\varphi(t)) \right) \right]_{\mathcal{Y}_i^\phi}, \quad (4b)$$

$$\underline{\mu}_i^\phi(t+1) = [\underline{\mu}_i^\phi(t) + \epsilon(v_i^\phi - v_i^\phi(t) - \eta \underline{\mu}_i^\phi(t))]_{+}, \quad (4c)$$

$$\bar{\mu}_i^\phi(t+1) = [\bar{\mu}_i^\phi(t) + \epsilon(v_i^\phi(t) - \bar{v}_i^\phi - \eta \bar{\mu}_i^\phi(t))]_{+}, \quad (4d)$$

$$\mathbf{v}(t+1) = \mathbf{R}\mathbf{p}(t+1) + \mathbf{X}\mathbf{q}(t+1) + \tilde{\mathbf{v}}, \quad (4e)$$

where (4a)–(4d) are for all  $\phi \in \Phi_i$  and all  $i \in \mathcal{N}$ . Proof of (4) converging asymptotically to its unique saddle point can be found in numerous references, e.g., [3], [6].

## III. MULTI-LEVEL OPF ALGORITHM

### A. Motivation

We have discussed the computational complexity of calculating the last coupling terms in (4a)–(4b) for a large network,

i.e.,  $\mathcal{O}(n^2)$ , and proposed a hierarchical (bi-level) algorithm to address this issue in our previous work [3]. Specifically, when we divide the large system geographically/administratively into areas featuring subtrees, we can take advantage of the network structure as well as the linearization model (1) to simplify the calculation of the computationally heavy coupling parts without compromising any performance based on the collaboration of divided areas. In this way, the computational efficiency has been significantly improved while nodal information within areas are preserved from outside of the area.

However, geographical/administrative division may leave certain areas to be large, in which case calculating the coupling terms are still heavy within such areas. Moreover, certain subareas within larger areas may want to preserve nodal information from the area. These motivate us to deploy the developed hierarchical techniques to the areas.

### B. Methods

1) *Design Intuition*: Because the sensitivity matrices  $\mathbf{R}$  and  $\mathbf{X}$  are built based on  $Z_{ij} = \sum_{(\zeta, \xi) \in \mathcal{E}_i \cap \mathcal{E}_j} z_{\zeta\xi}^{\varphi-\phi}$  that depends on the common path of bus  $i$  and  $j$  to the substation, i.e.,  $\mathcal{E}_i \cap \mathcal{E}_j$ , and that two non-overlapping subtrees hold the same  $\mathcal{E}_i \cap \mathcal{E}_j$  for any of their respective buses  $i$  and  $j$ , we conclude that,

$$\partial_{p_j^\phi} v_i^\varphi = \partial_{p_{n_h^0}^\phi} v_{n_k^0}^\varphi = 2\Re\{\bar{Z}_{n_k^0 n_h^0}^{\varphi-\phi} \cdot \omega^{\varphi-\phi}\} \quad (5a)$$

$$\partial_{q_j^\phi} v_i^\varphi = \partial_{q_{n_h^0}^\phi} v_{n_k^0}^\varphi = -2\Im\{\bar{Z}_{n_k^0 n_h^0}^{\varphi-\phi} \cdot \omega^{\varphi-\phi}\} \quad (5b)$$

hold for any  $i \in \mathcal{N}_k$  and any  $j \in \mathcal{N}_h$ , where  $\mathcal{N}_k$  and  $\mathcal{N}_h$  respectively denote the sets collecting buses of two non-overlapping subtrees indexed by  $k, h \in \mathcal{K}$  with their respective root buses indexed by  $n_k^0$  and  $n_h^0$ , with set  $\mathcal{K}$  collecting all subtree indexes. See Fig. 1 for an illustration, where the white dashed line is the common path of any node in Area 1 and any node in Area 3—marked by blue triangles—to the substation. Because subtrees inherit all features from the original tree, we can apply similar results to them. Due to space limit, we refer to [3], [7] for more details.

2) *Multi-Level Implementation*: Based on such intuition, we can equivalently rewrite the last term of (4a) for clustered node  $i \in \mathcal{N}_k$  with phase  $\phi \in \Phi_i$  as the follows three parts (the last term in (4b) can be processed similarly):

$$2\Re\left\{ \sum_{\varphi \in \Phi_0} \omega^{\varphi-\phi} \sum_{j \in \mathcal{N}^\varphi \cap \mathcal{N}_k} \bar{Z}_{ji}^{\varphi-\phi} (\bar{\mu}_j^\varphi(t) - \underline{\mu}_j^\varphi(t)) \right\} + \quad (6a)$$

$$2\Re\left\{ \sum_{\varphi \in \Phi_0} \omega^{\varphi-\phi} \sum_{\substack{n_h^0 \in \mathcal{N}^\varphi \\ h \in \mathcal{K}, h \neq k}} \bar{Z}_{n_h^0 n_k^0}^{\varphi-\phi} \sum_{j \in \mathcal{N}^\varphi \cap \mathcal{N}_h} (\bar{\mu}_j^\varphi(t) - \underline{\mu}_j^\varphi(t)) \right\} + \quad (6b)$$

$$2\Re\left\{ \sum_{\varphi \in \Phi_0} \omega^{\varphi-\phi} \sum_{j \in \mathcal{N}^\varphi \cap \mathcal{N}_0} \bar{Z}_{jn_k^0}^{\varphi-\phi} (\bar{\mu}_j^\varphi(t) - \underline{\mu}_j^\varphi(t)) \right\}. \quad (6c)$$

Here, (6b) significantly simplifies the original computation by reducing a large number of repetitive computations by applying the result in (5a), and (6c) captures the influence from buses outside any divided subtree area (e.g., Area 5 in Fig. 1) whose buses are collected in set  $\mathcal{N}_0$  for completeness.

Look at (6a) and we notice that it has a similar form as the original coupling term. Hence, the computational complexity  $\mathcal{O}(|\mathcal{N}_k|^2)$  for (6a) can be high for large  $|\mathcal{N}_k|$ . Fortunately, we can apply similar tricks to divide area  $\mathcal{N}_k$  into subtrees

Bi-Level Algorithm [3]	Areas		Area 1				Area 2				Area 3				Area 4	Total
	Loads #		357				222				310				154	1043
	Time (s)		1050.16				501.21				834.90				256.81	2717.25
Tri-Level Algorithm	Subareas	1 <sub>1</sub>	1 <sub>2</sub>	1 <sub>3</sub>	1 <sub>0</sub>	2 <sub>1</sub>	2 <sub>2</sub>	2 <sub>3</sub>	2 <sub>0</sub>	3 <sub>1</sub>	3 <sub>2</sub>	3 <sub>3</sub>	3 <sub>0</sub>	4 <sub>0</sub>	Total	
	Loads #	49	74	23	211	70	39	17	96	68	66	68	108	154	1043	
	Time (s)	713.08 (32% faster)				337.04 (33% faster)				490.51(41% faster)				261.07	1890.40 (30% faster)	

TABLE I: Detailed clustering information and computational time of all areas and subareas under 3,000 iterations.

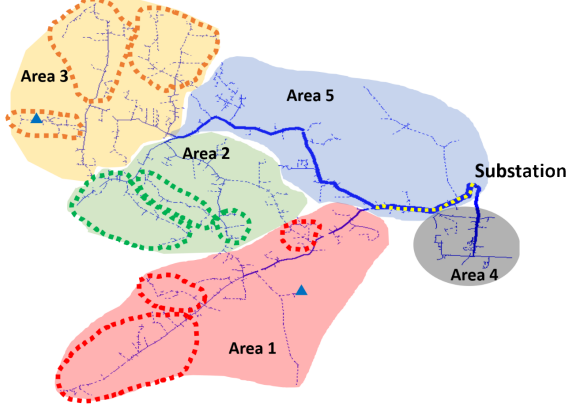


Fig. 1: Areas and subareas (within dashed lines) of the network used in Section IV.

indexed by  $k_m \in \mathcal{K}_k = \{k_1, k_2, \dots\}$  and their corresponding buses sets denoted by  $\mathcal{N}_{k_m}$  together with  $\mathcal{N}_{k_0}$  collecting the remaining buses. We then equivalently rewrite (6a) for  $i \in \mathcal{N}_{k_m} \subset \mathcal{N}_k, m \in \mathcal{K}_k, k \in \mathcal{K}$  as

$$2\Re\left\{ \sum_{\varphi \in \Phi_0} \omega^{\varphi-\phi} \sum_{j \in \mathcal{N}^{\varphi} \cap \mathcal{N}_{k_m}} \bar{Z}_{ji}^{\varphi\phi} (\bar{\mu}_j^{\varphi}(t) - \underline{\mu}_j^{\varphi}(t)) \right\} + \quad (7a)$$

$$2\Re\left\{ \sum_{\varphi \in \Phi_0} \omega^{\varphi-\phi} \sum_{\substack{n_{k_m}^0 \in \mathcal{N}^{\varphi} \\ k'_m \in \mathcal{K}_k, m' \neq m}} \bar{Z}_{n_{k_m}^0 n_{k'_m}^0}^{\varphi\phi} \sum_{j \in \mathcal{N}^{\varphi} \cap \mathcal{N}_{k'_m}} (\bar{\mu}_j^{\varphi}(t) - \underline{\mu}_j^{\varphi}(t)) \right\} + \quad (7b)$$

$$2\Re\left\{ \sum_{\varphi \in \Phi_0} \omega^{\varphi-\phi} \sum_{j \in \mathcal{N}^{\varphi} \cap \mathcal{N}_{k_0}} \bar{Z}_{jn_{k_0}^0}^{\varphi\phi} (\bar{\mu}_j^{\varphi}(t) - \underline{\mu}_j^{\varphi}(t)) \right\}, \quad (7c)$$

where  $n_{k_m}^0$  denotes the root bus of subtree  $k_m$ . Now (7b) further simplifies the computation for (6a) similarly as (6b) does for (4a). Note that nodal information within subtrees are aggregated without being exposed.

By considering the fractal properties of tree/subtree, i.e., subtrees have tree structures and thus can be further divided into subtrees where everything still holds, such layering structure can be theoretically adapted as deep as we wish, if it is needed and if the network allows.

#### IV. NUMERICAL RESULTS

We construct a three-phase unbalanced, 11,000-node test feeder by connecting an IEEE 8,500-node test feeder and an EPRI Ckt7 test feeder at the substation. We simplify the network by lumping the loads on the secondary side into corresponding distribution transformers, resulting in a 4,521-node network ( $N = 4,521$ ) with 1,043 controllable loads. We group all the controllable nodes into four subtree areas, and divide Areas 1–3 further into subareas featuring subtrees and remaining buses; see Fig. 1 and Table I. The simulation runs with Python 3.6 on Windows 10 Enterprise Version on a laptop with Intel Core i7-7600U CPU @ 2.80GHz 2.90GHz,

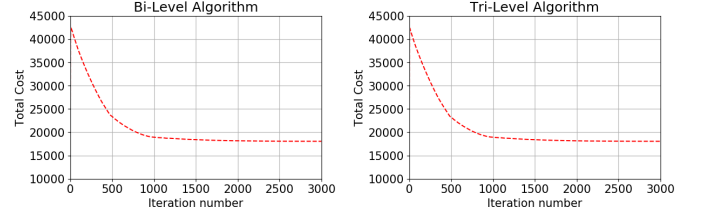


Fig. 2: The bi-level and tri-level algorithms exhibit identical convergence dynamics to the same minimum cost.

8.00GB RAM. OpenDSS is used to simulate the nonlinear power flow.

As shown in Fig. 2, by adding one additional layer of hierarchical implementation, the tri-level algorithm does not change the convergence dynamics or minimum cost value at convergence from the bi-level algorithm. Meanwhile, because of the computational complexity reduced from the bi-level algorithm to tri-level algorithm, i.e., by equivalently replacing (6a) with (7), it takes less computational time in each areas (see TABLE I) and 30% less time in total for the tri-level algorithm to complete the 3,000 iterations towards convergence. Note that Area 4 has similar computational time under two cases because we do not have subareas for it.

Such computational complexity reduction without compromising optimality gives us “free” speed improvement. Moreover, the multi-level structure also allows for more parallel and autonomous implementation among areas and subareas and potentially further speeds up the convergence. We also refer to numerical results in [3] for 4-time “free” speed improvement from centralized (one-level) implementation to bi-level implementation for the interested readers.

#### V. CONCLUSION

By exploring the fractal properties of power distribution networks of tree topology, this letter extends our previous bi-level distributed OPF solver based on gradient algorithm to multi-level implementation. Numerical results on a 4,521-node large network show significant computational speed improvement of such extension without compromising optimality.

#### REFERENCES

- [1] D. K. Molzahn, F. Dörfler, H. Sandberg, S. H. Low, S. Chakrabarti, R. Baldick, and J. Lavaei, “A survey of distributed optimization and control algorithms for electric power systems,” *IEEE Trans. on Smart Grid*, vol. 8, no. 6, pp. 2941–2962, 2017.
- [2] B. Kroposki, E. Dall’Anese, A. Bernstein, Y. Zhang, and B.-M. Hodge, “Autonomous energy grids,” *Proc. of Hawaii International Conference on System Sciences*, 2018.
- [3] X. Zhou, Z. Liu, C. Zhao, and L. Chen, “Accelerated voltage regulation in multi-phase distribution networks based on hierarchical distributed algorithm,” *IEEE Trans. Power Systems*, 2019.

- [4] L. Gan and S. H. Low, "Convex relaxations and linear approximation for optimal power flow in multiphase radial networks," *Proc. of Power Systems Computation Conference (PSCC)*, pp. 1–9, 2014.
- [5] L. Gan and S. H. Low, "An online gradient algorithm for optimal power flow on radial networks," *IEEE Journal on Selected Areas in Communications*, vol. 34, no. 3, pp. 625–638, 2016.
- [6] D. P. Bertsekas and J. N. Tsitsiklis, *Parallel and distributed computation: numerical methods*. Prentice hall Englewood Cliffs, NJ, 1989, vol. 23.
- [7] X. Zhou, Z. Liu, Y. Guo, C. Zhao, and L. Chen, "Gradient-based multi-area distribution system state estimation," *arXiv preprint arXiv:1909.11266*, 2019.